International Journal of Bioprinting

REVIEW ARTICLE

Advances in 3D printing techniques for cartilage regeneration of temporomandibular joint disc and mandibular condyle

Shoushan Hu[1,2], Yating Yi[1,2], Chengxinyue Ye[1,2], Jin Liu[1]*, Jun Wang[2]*

[1]Lab for Aging Research, State Key Laboratory of Biotherapy and National Clinical Research Center for Geriatrics, West China Hospital, Sichuan University, Chengdu 610041, China

[2]State Key Laboratory of Oral Diseases & National Clinical Research Center for Oral Diseases & Department of Orthodontics, West China Hospital of Stomatology, Sichuan University, Chengdu 610041, China

(This article belongs to the *Special Issue: 3D Printing of Cartilage-Mimicking Constructs: Targeting the Functional Regeneration of Tissue Anatomy and Physiology*)

Abstract

Temporomandibular joint (TMJ) osteoarthritis causes fibrocartilage damage to the TMJ disc and mandibular condyle, resulting in local pain and functional impairment that further reduces patients' quality of life. Tissue engineering offers a potential treatment for fibrocartilage regeneration of the TMJ disc and mandibular condyle. However, the heterogeneous structure of TMJ fibrocartilage tissue poses significant challenges for the fabrication of biomimetic scaffolds. Over the past two decades, some researchers have attempted to adopt three-dimensional (3D) printing techniques to fabricate biomimetic scaffolds for TMJ fibrocartilage regeneration, but publications on such attempts are limited and rarely report satisfactory results, indicating an urgent need for further development. This review outlines several popular 3D printing techniques and the significant elements of tissue-engineered scaffolds: seed cells, scaffold materials, and bioactive factors. Current research progress on 3D-printed scaffolds for fibrocartilage regeneration of the TMJ disc and mandibular condyle is reviewed. The current challenges in TMJ tissue engineering are mentioned along with some emerging tissue-engineering strategies, such as machine learning, stimuli-responsive delivery systems, and extracellular vesicles, which are considered as potential approaches to improve the performance of 3D-printed scaffolds for TMJ fibrocartilage regeneration. This review is expected to inspire the further development of 3D printing techniques for TMJ fibrocartilage regeneration.

Keywords: 3D printing; Cartilage regeneration; Temporomandibular joint disc; Mandibular condyle

***Corresponding authors:**
Jin Liu (liujin@scu.edu.cn)

Jun Wang
(wangjunv@scu.edu.cn)

Citation: Hu S, Yi Y, Ye C, *et al*., 2023, Advances in 3D printing techniques for cartilage regeneration of temporomandibular joint disc and mandibular condyle. *Int J Bioprint,* 9(5): 761.
https://doi.org/10.18063/ijb.761

Received: February 12, 2023
Accepted: March 31, 2023
Published Online: May 25, 2023

1. Introduction

Temporomandibular joint (TMJ) is a synovial joint composed of the mandibular condyle, temporal fossa, and articular disc, whereas the TMJ cartilage is composed of fibrocartilage, which is distinct from hyaline cartilage[1]. TMJ osteoarthritis is defined as a degenerative and low-inflammatory disease in the unilateral or bilateral TMJ,

which affects 9.8% of the adult and elderly population[2,3]. Among the complicated etiological factors of TMJ osteoarthritis, the fundamental cause is assumed to be the excessive mechanical loading on the healthy or impaired articular fibrocartilage, which may result from mandibular asymmetry, severe malocclusion, and muscle overuse[4]. Locally, the excessive mechanical loading would lead to both displacement and impairment of the TMJ disc and progressive osteochondral defects of the mandibular condyle[5], with flattening and erosion of the articular surface as the typical morphologic changes on the cone beam computed tomography[6]. The typical pathological change in the fibrocartilage tissue in the early phase of TMJ osteoarthritis is chondrocyte apoptosis or necrosis, along with the overexpression of inflammatory cytokines in the synovial fluid of patients[7]. As TMJ osteoarthritis progresses, patients may exhibit orofacial pain, mouth-opening limitation, and joint clicking sound as common clinical symptoms, affecting swallowing, speaking, and other orofacial activities[7].

Treatment alternatives for TMJ osteoarthritis are primarily divided into non-surgical and surgical options, depending on the severity of the case[2]. For TMJ osteoarthritis patients with mild pain and clicking sounds, conservative treatment, such as arthrocentesis with/without hyaluronic acid injection, occlusal splints, and non-steroidal anti-inflammatory drugs, aiming to relieve pain and pathological progress is recommended[7]. When local inflammation has severely impaired most of the TMJ anatomical structure and caused intractable pain, surgical intervention would be the priority treatment option. Functional restoration of the TMJ can be achieved by joint replacement using an autologous bone, such as costochondral grafts and free fibula flaps, or an artificial joint[8]. Autologous cartilage transplantation, on the other hand, would pose additional lesions and risk of complications at the donor site. Allogeneic cartilage transplantation avoids the donor site lesion but has limited application due to the risk of immune rejection[9]. Regarding the long-term treatment effects of TMJ prosthesis, postoperative complications, such as metal particulation leading to osteolysis, have been reported, and therefore, patients treated by TMJ prosthesis have to take the risk of revision surgery[10]. Considering that the need for physiological reconstruction of TMJ condyle and disc remains unmet based on the existing treatment regimen, cartilage tissue engineering has garnered increasing attention as a promising alternative for TMJ fibrocartilage defects.

With progressive achievements in biomaterials and regenerative medicine, cartilage tissue engineering has been increasingly explored. The primary process of cartilage tissue engineering is to select one or some specific cells as seed cells, and inoculate them with bioactive additives on biodegradable scaffolds to form artificial grafts, which are transplanted into the cartilage defect[11]. Degradation of the scaffold material occurs simultaneously with cell proliferation and cartilage matrix secretion, resulting in the formation of new cartilage and local anatomical structures. However, the complex heterogeneous structures of the TMJ disc and mandibular condyle pose great challenges to the fabrication of biomimetic tissue structures based on traditional scaffold-based strategies. Notably, three-dimensional (3D) printing has emerged in recent years as a promising technique, which allows precise control of the internal structure and dimensional parameters of scaffolds to fabricate bionic scaffolds for articular cartilage regeneration[12]. Unfortunately, in some reviews on TMJ regenerative medicine, the content related to 3D-printed scaffolds for TMJ tissue regeneration was very limited and thus did not fully present the great potential of 3D-printed scaffolds[13,14]. On the other hand, several reviews focusing on 3D printing technology in various cartilage tissue-engineering fields, such as knee joint, meniscus, intervertebral disc, ear and nose, etc., have been published recently, while reviews on 3D-printed scaffolds for TMJ fibrocartilage regeneration are lacking[12,15-18]. With the increasing popularity of 3D printing techniques in tissue engineering and regenerative medicine, the great potential of 3D-printed scaffolds for TMJ fibrocartilage regeneration should not be ignored. Therefore, in this review, we will briefly introduce some popular 3D printing techniques and a scaffold design framework, and then summarize the research progress of 3D-printed scaffolds for TMJ fibrocartilage regeneration, followed by some current challenges and emerging tissue-engineering strategies, which are potential approaches to improve the performance of 3D-printed scaffolds.

2. 3D printing techniques for cartilage tissue engineering

The initial step in the 3D printing process to achieve articular cartilage regeneration is to scan the biological tissue or organ with computed tomography and magnetic resonance imaging and build 3D models based on the acquired data of the tissue characteristics. Then, appropriate biomaterials are adopted to fabricate scaffolds using 3D printing techniques. Seed cells are cultured with specific bioactive factors (BFs) and then seeded into the 3D-printed scaffolds to enhance their performance. Another strategy is to fabricate the bioink consisting of seed cells, BFs, and scaffold materials[19]. A 3D bioprinter under the control of computer can convert the obtained data into a 3D-printed scaffold using bioink. Subsequently, *in vitro* culture will accelerate the maturation and promote

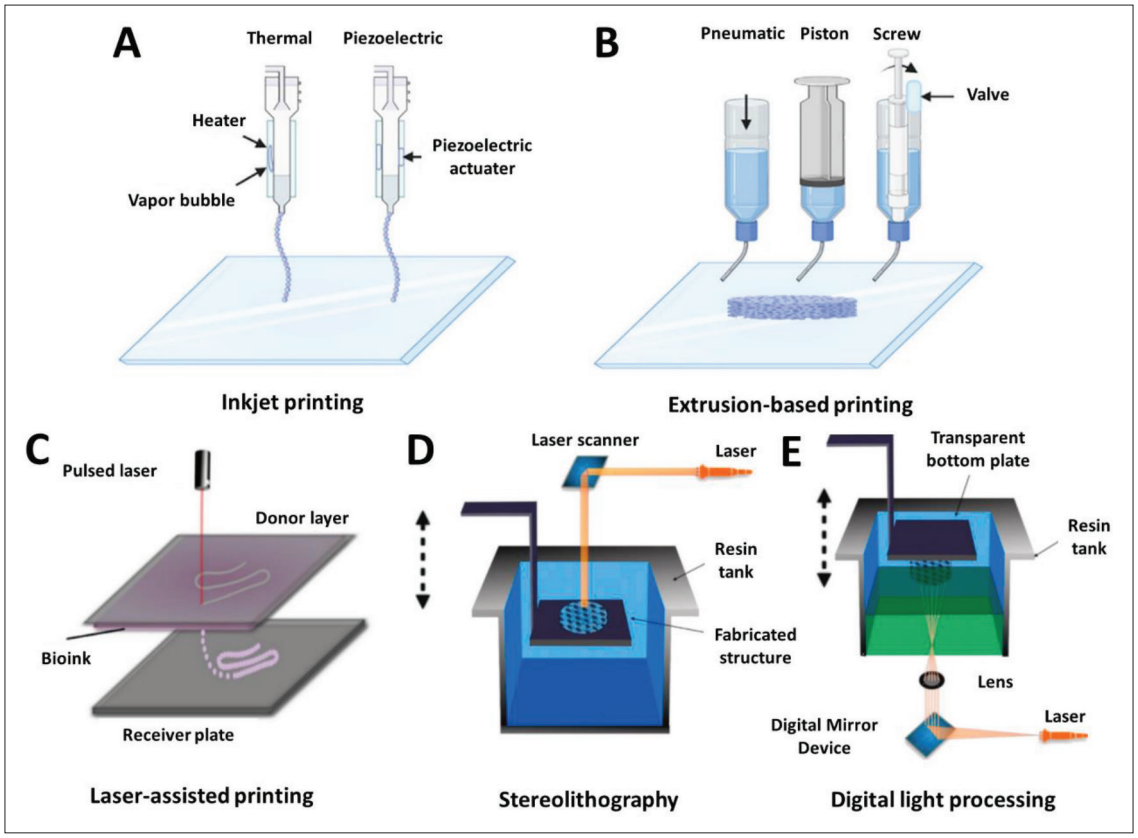

Figure 1. Schematic diagram of different 3D printing techniques supporting bioink. (A) Inkjet printing. (B) Extrusion-based printing (EBP). (from ref.[19] licensed under Creative Commons Attribution license). (C) Laser-assisted printing (LAP). Reproduced with permission from Ravanbakhsh H, Karamzadeh V, Bao G, *et al.*, Adv Mater, Copyright © 1999-2023 John Wiley & Sons[41]. (D) Stereolithography. (E) Digital light processing. (from ref.[37] licensed under Creative Commons Attribution-NonCommercial-NoDerivatives 4.0 license).

the biological properties of the artificial scaffold, which is then transplanted to the tissue defect site *in vivo*. Compared with the traditional 3D printing techniques, some 3D printing techniques supporting bioink have greater potential in cartilage tissue engineering and have gained growing popularity in recent years, and some of them are introduced below (Table 1).

2.1. Inkjet printing

Inkjet printing technology is characterized by low-cost, high printing speed, relatively high cell viability, and combined use of bioinks with different properties (Figure 1A)[20]. During the electronically controlled printing process, the bioink is squeezed into micron-scale droplets at the printer head by a thermal or piezoelectric actuator. The droplets of a controllable size are sprayed onto the substrate, and the tailored 3D structure is generated by layer-by-layer deposition of bioink[21]. The thermal inkjet system and the piezoelectric inkjet system differ in their operating principles and characteristics. In a thermal inkjet system, a tiny heating element near the nozzle rapidly heats up to 200–300°C in a few microseconds to form bubbles, which then expand and push the bioink out of the nozzle to form droplets[22]. The bioink used for thermal inkjet printing must be thermally stable, which limits the choice of bioink. Compared with thermal inkjet printing, piezoelectric inkjet printing generates a pressure pulse inside the nozzle by a piezoelectric element, thus avoiding potential adverse effects on cells in the bioink from the thermal stress. However, it is difficult for the thermal/piezoelectric inkjet system to print with bioinks with high viscosity or high cell density due to nozzle clogging[23]. In recent years, the acoustic droplet ejection technology has been developed, which forms droplets by acoustic energy and has the advantage of protecting the printheads from clogging by manipulating the droplet size[24].

2.2. Extrusion-based printing

The principle of the extrusion-based printing (EBP) technique is that the pneumatic, piston, or screw-driven device generates continuous pressure to extrude the bioink from the nozzle to form filaments, which are deposited on the platform to form a 3D structure (Figure 1B)[25]. Several variations of EBP strategies have been developed

Table 1. Comparison of different 3D printing techniques in cartilage tissue engineering

3D printing techniques	Sub-category	Advantages	Disadvantages	References
Inkjet printing	• Thermal inkjet printing • Piezoelectric inkjet printing • Acoustic droplet ejection	• Low cost • High cell viability (75%–95%) • High print resolution • Support multi-material	• Easy nozzle clogging • Limited bioink viscosity • Low cell density (<10^6 cells/mL)	[20-24]
Extrusion-based printing	• Embedded printing • Co-axial printing • Multi- or single-nozzle multi-material printing • Continuous chaotic printing	• High bioink viscosity • High cell density (>10^8 cells/mL) • Suitable for multi-material and various printing demands	• Low cell viability (40%–80%) • Moderate resolution	[25-32]
Laser-assisted printing	-	• High cell viability (>95%) • High bioink viscosity • High print resolution	• Low cell density (<10^6 cells/mL) • High cost • Complex control system	[23,30,33,35,36]
Vat photopolymerization	• Stereolithography • Digital light processing	• High cell viability (>85%) • High print resolution	• Only support liquid photosensitive materials	[30,32,37,40]

to meet different printing requirements, such as embedded printing, co-axial printing, multi- or single-nozzle multi-material printing, and continuous chaotic printing[26]. For example, single-nozzle multi-material printing allows the synchronized delivery of different bioinks with an array of nozzles to fabricate the product with heterogeneous materials and gradient hierarchical structures[27]. In addition, the fabrication of multi-material core-shell structures that mimic anatomical tissues can be easily achieved by co-axial printing[28]. The nozzle size can be adjusted by computer to realize the control of the printing resolution[29]. However, compared with other 3D printing technologies, the printing resolution of the EBP is lower, resulting in poorer accuracy of cell organization[30]. The reduction in nozzle diameter may place greater shear stress on the cells, resulting in a decrease in cell viability[31]. Despite such drawbacks as limited resolution and lower cell activity, EBP is still widely applied due to fast printing speed, ease of implementation, and support for a wide range of bioinks, especially bioinks with high cell density or high viscosity[32].

2.3. Laser-assisted printing

Laser-assisted printing (LAP) is a nozzle-free printing approach that avoids technical problems associated with the printhead, such as nozzle clogging. LAP is composed of a pulsed laser source, a donor slide, and a receiver slide (Figure 1C)[33]. The donor slide consists of three layers from top to bottom, which are made of transparent glass, metal, and bioink, respectively. The working principle of LAP is derived from laser-induced forward transfer technology, which was introduced over 30 years ago[34]. The ultraviolet (UV) light from a pulsed laser source projects onto the energy-absorbing layer (metal layer) of the donor slide and causes local vaporization. The vaporization-induced bubbles push the bioink layer on the lower part of the donor slide to form droplets, which are deposited on the receiving substrate and quickly crosslinked[35]. In the non-contact printing process, cell viability can be protected by adjusting the thickness of the metal film[36]. Moreover, cells are free from either thermal or mechanical stress, thus maintaining a relatively high cell activity (>95%)[23]. By adjusting the parameters of the laser pulse, high-precision printing of bioinks with different viscosities can be achieved. However, compared with nozzle-based printing technology, the high cost and complex control system limit the application of LAP[30].

2.4. Vat photopolymerization

Vat photopolymerization (VPP) 3D printing includes stereolithography (Figure 1D) and digital light processing (Figure 1E)[37]. The principle of stereolithography is that the liquid photosensitive bioink is photopolymerized in a vat under exposure to UV light. After the computer-

controlled laser completes the bioink solidification on the surface layer, the vat is lowered. The next layer is crosslinked at the top of the previous section, and layer-by-layer solidification eventually forms a 3D model[32]. In contrast to stereolithography, in the course of digital light processing, UV light projects a 2D pattern onto the surface of the liquid resin material through a digital micromirror device[38]. With the vertical movement of the substrate, the liquid resin material is solidified layer by layer until a designed structure is constructed[39]. VPP prevents cells from physical stress, thus maintaining high cell viability and supporting high printing resolution[40]. However, VPP is only applicable to liquid photosensitive materials, which limits its application scope[30]. In the past decade, several strategies of VPP have been developed to fabricate multi-material constructs, including multi-vat, sequential injection, sequential deposition, and multi-wavelength, thus increasing the potential of VPP for tissue-engineering applications[41].

3. Scaffold components

3.1. Seed cell

Due to the lack of blood vessels and nerves, articular cartilage tissue has insufficient self-repair capacity. Therefore, seed cells are required to have the ideal ability to proliferate and secrete extracellular matrix (ECM). Seeding techniques such as static seeding, negative pressure seeding, centrifugal seeding, spinner flask, orbital shaker, and perfused bioreactor can be used to seed cells onto the scaffolds to promote articular cartilage regeneration[42-44]. The commonly used seed cells in cartilage tissue engineering and the effects of cell density in the scaffolds will be discussed below.

Mature chondrocytes as part of cartilage tissue can be cultured *in vitro*, then inoculated onto 3D-printed artificial scaffolds, and ultimately transplanted into the defect site to promote articular cartilage regeneration. The feasibility of this regimen has been verified on mature chondrocytes from various sources, including humans, bovine, rabbits, etc.[12] Specifically, compared with tissue-engineered constructs with articular chondrocytes, tissue-engineered constructs with costal chondrocytes showed greater glycosaminoglycan (GAG)/wet weight and tensile strength, suggesting a better tissue-engineering potential of costal chondrocytes in TMJ fibrocartilage regeneration[45]. Furthermore, the passaged costal chondrocytes were demonstrated to have potential superiority over primary costal chondrocytes in TMJ fibrocartilage tissue engineering, as the former produced more GAG than the latter *in vitro*[46]. An *in vivo* study further confirmed the ability of the passaged costal chondrocytes in TMJ disc repair[47]. Chondrocytes co-cultured with other types of cells have been demonstrated to be a feasible strategy in TMJ fibrocartilage tissue engineering, such as fibrochondrocytes and articular chondrocytes[48]. The limited availability of tissue and dedifferentiation tendency during *in vitro* culture are assumed to be the main challenges of mature chondrocytes as seed cells in application[12].

Mesenchymal stem cells (MSCs) have been widely used as seed cells in TMJ fibrocartilage tissue engineering due to their great ability of differentiation, proliferation, and ECM secretion. Extensive research has demonstrated the potential of MSCs from bone marrow, adipose tissue, and synovial fluid for TMJ fibrocartilage tissue engineering[49]. Continuous attempts have been made to explore more seed cells suitable for TMJ fibrocartilage tissue engineering. It has been reported that dental pulp stem cells (DPSCs) seeded on the scaffold were cultured in chondrogenic media for 8 weeks, resulting in increased gene expression of fibrocartilaginous markers[50]. In addition, umbilical cord MSCs[51], induced pluripotent stem cells (iPSCs)[52], periodontal ligament stem cells (PDLSCs)[53], and deciduous teeth stem cells (DTSCs)[54] have been demonstrated as potential seed cells in TMJ regenerative medicine.

The effect of cell density on cell behavior and scaffold properties should not be ignored. Excessive cell density may lead to a decrease in the ability of individual cells to secrete ECM and prolong the expansion cycle of cell culture *in vitro*, while low cell density may not be conducive to cell differentiation and secretion of ECM[55]. The density of articular chondrocytes is distributed in a density gradient, gradually decreasing from superficial to deep[56]. To mimic natural articular cartilage, cell density gradient scaffolds were fabricated and it was demonstrated that ECM production was positively correlated with cell density[57,58]. Furthermore, the comparison of the scaffolds seeded with different initial cell densities showed that the compressive stiffness, modulus, thickness, and wet weight as well as GAG and collagen content of the cartilaginous constructs increased with increasing cell density[59]. A recent review summarized that the cell density in the majority of bioinks for articular cartilage repair ranged from 5 to 20×10^6 cells/mL[12]. Under the specific conditions, desirable results can also be achieved by the scaffolds with the cell densities of 25×10^6 cells/mL[60], 50×10^6 cells/mL[61], 60×10^6 cells/mL[62], and so on. So far, there is no gold standard for optimal cell density because it depends on cell type, scaffold biomaterial, BFs, and culture conditions. Therefore, it is suggested to compare the effects of the combination of the specific scaffold and multiple cell densities to determine the appropriate cell density for the specific scaffold.

3.2. Scaffold biomaterial

Artificial scaffolds with biocompatibility and biodegradability are required to have mechanical properties similar to

those of articular cartilage tissue, including hardness, viscoelasticity, compressive modulus, shear stress, etc. Artificial scaffolds serve to bear loading and remain intact after implantation into the cartilage defect, providing space for cell differentiation, proliferation, and ECM secretion. As the local tissue regenerates, the artificial scaffold degrades at an appropriate rate, leaving no toxic residue. A recent review compared the properties and limitations of different biomaterials in cartilage tissue engineering[30]. Scaffold materials can be broadly categorized into two groups: natural biomaterials and synthetic biomaterials, both of which are briefly discussed below.

There has been a wealth of research on natural biomaterials in cartilage tissue engineering, including collagen, silk fibroin, fibrin, gelatin, sodium alginate (SA), hydroxyapatite (HA), hyaluronic acid (HyA), agarose, chitosan, chondroitin sulfate, and decellularized extracellular matrix (dECM)[12,30,63]. Despite ideal biocompatibility and cytocompatibility, natural biomaterials innately possess several flaws, such as poor mechanical properties, poor thermal stability, inappropriate degradation rate, etc. Several strategies have been proposed to overcome the obstacles. Compared with the 3D-printed scaffolds with SA alone, those with the combination of SA and type I collagen exhibited higher mechanical strength and effectively suppressed the dedifferentiation tendency of chondrocytes[64]. In addition, physical and chemical modifications have been adopted as an effective approach to impart favorable 3D printing properties to the natural biomaterials (collagen, HyA, chondroitin sulfate, and dECM)[12].

Common synthetic biomaterials include polyvinyl alcohol (PVA), polyethylene glycol (PEG), polycaprolactone (PCL), polyurethane (PU), polyglycolic acid (PGA), poly (D, L-lactic-co-glycolic acid) (PLGA), and poly (lactic acid) (PLA)[29,30,63]. Compared with natural biomaterials, synthetic biomaterials are gaining popularity due to their advantages such as better printability, structural stability, controlled mechanical property, and degradation rate. However, some undesirable properties of synthetic materials, such as bioinert and slow degradation rate, are not conducive to articular cartilage regeneration[15]. Recent attempts to combine natural and synthetic biomaterials to fabricate hybrid scaffolds provide an effective approach to improve scaffold performance[65-67]. For instance, the PCL scaffolds modified with chitosan hydrogel were more conducive to the adhesion and proliferation of synovial MSCs than PCL scaffolds[67].

3.3. Bioactive factor

Growth factors (GFs), mineral ions, and intracellular signaling molecules are collectively referred to BFs, which play a vital role in articular cartilage regeneration. BFs can be loaded onto the scaffolds by direct blending or soaking, surface coating, embedding micro-nano particles, etc. to enhance the scaffold performance, such as promoting cell growth, differentiation, and proliferation, and benefiting ECM production and homeostasis[68]. In previous research, BFs used to promote cartilage regeneration included bone morphogenetic proteins (BMP), fibroblast growth factor (FGF), transforming growth factor beta (TGF-β), insulin growth factor (IGF), NEL-like molecule-1 (NELL-1), platelet-derived growth factor (PDGF), epidermal growth factor (EGF), SOX family of transcription factors, interleukin 1 (IL-1), vascular endothelial growth factor (VEGF), hepatocyte growth factor (HGF), connective tissue growth factor (CTGF), and tumor necrosis factor alpha (TNF-α)[12,30,63,69]. Platelet-rich plasma (PRP) is a common source of BFs, containing IGF-1, PDGF, FGF, and TGF-β1[12]. PRP can also be incorporated into bioink to form a 3D-printed scaffold that serves to promote chondrogenic differentiation of MSCs and deposition of ECM components[70]. In addition, the combined application of multiple BFs exerts a synergistic effect in promoting TMJ fibrocartilage regeneration, such as CTGF, BMP-2 and TGF-β3[71], BMP-2 and TGF-β1[72]. In general, screening for the optimal combination of seed cells, BFs, and scaffold materials is one of the research foci in TMJ fibrocartilage tissue engineering, and further investigations are needed (Figure 2).

4. TMJ disc cartilage tissue engineering

4.1. Anatomy

The TMJ disc is located in the joint capsule between the glenoid fossa and the mandibular condyle, ensuring that the mandibular condyle slides smoothly anteriorly and posteriorly during mouth opening and closing (Figure 3A). The morphological appearance of the TMJ disc is a biconcave and roughly-oval fibrocartilaginous plate, with a medial–lateral axis averaging 2.36 ± 0.0609 cm and an anterior–posterior axis averaging 1.40 ± 0.149 cm (Figure 3B)[73]. The collagen fibers form a ring around the periphery of the disc and are aligned anteroposteriorly throughout the intermediate band (Figure 3C)[1]. The TMJ disc can be divided into four sections: an anterior band (approximately 2 mm thick), an intermediate band (approximately 1 mm thick), a posterior band (approximately 3 mm thick), and a posterior bilaminar region[1]. Water, collagen, and GAG are three major components of the TMJ disc, accounting for 74.5 ± 4.2% wet weight, 62.0 ± 11.4% dry weight, and 3.2 ± 1.4% dry weight, respectively[74]. The distribution characteristics of the three components and the different biomechanical properties in different regions were mentioned in the previous research[74].

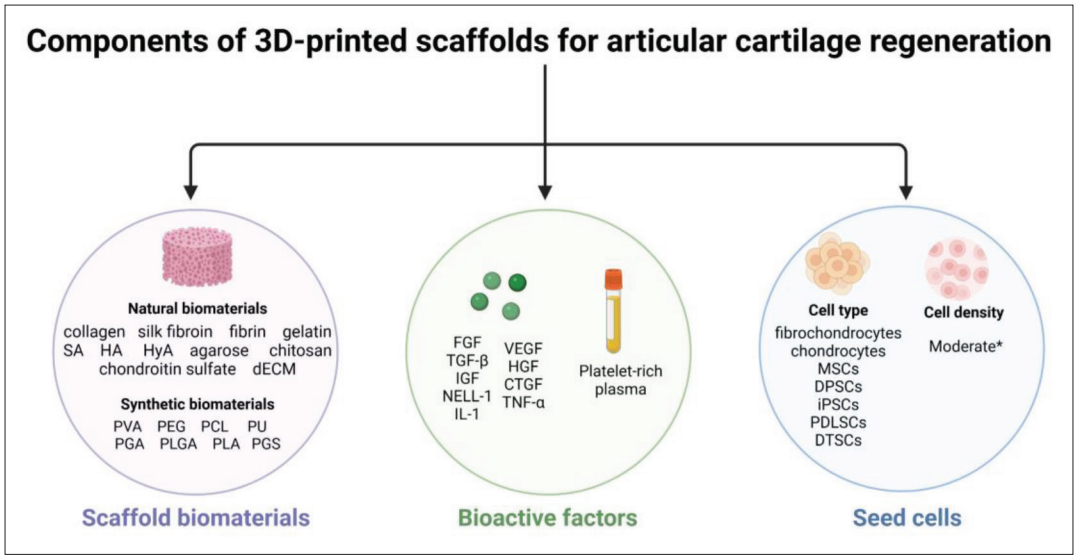

Figure 2. Schematic diagram of components of 3D-printed scaffolds for articular cartilage regeneration. *, too low or too high cell density is not advisable due to their undesirable effects on the cell behavior and scaffold performance; therefore, it is suggested to compare the effects of specific scaffolds with multiple cell densities to determine the appropriate cell density for the specific scaffolds.

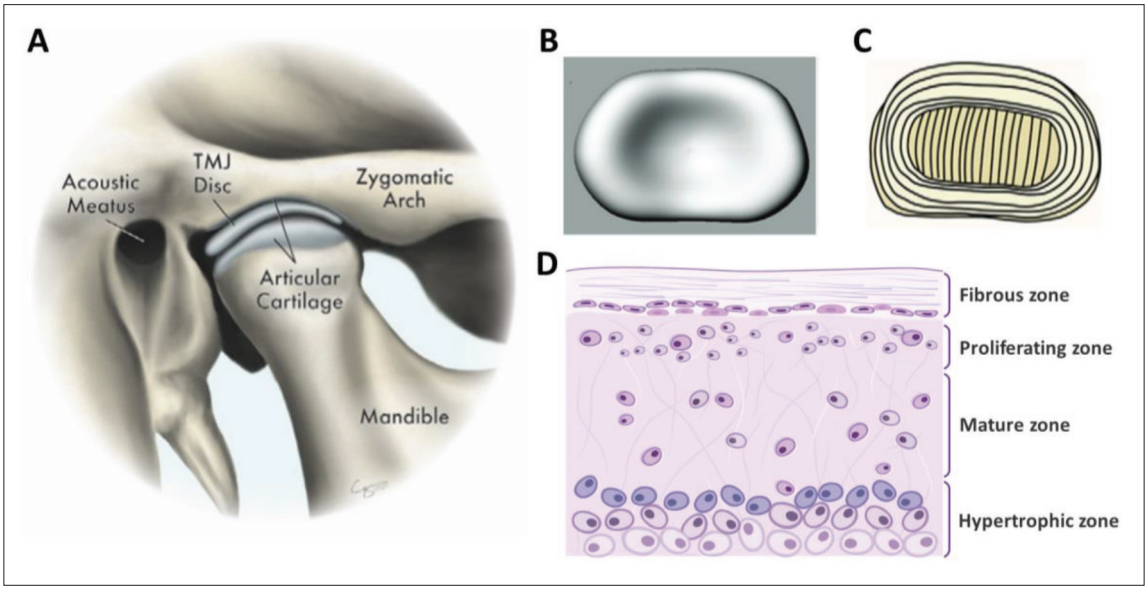

Figure 3. Anatomy of temporomandibular joint (TMJ). (A) Human TMJ sagittal schematic. (from ref.[95] licensed under Creative Commons Attribution license). (B) A 3D computer-aided design model of human TMJ. Reproduced with permission from Legemate K, Tarafder S, Jun Y, *et al.*, *J Dent Res*, 95: 800–7[75]. (C) Schematic diagram showing the arrangement of the collagen fibers in TMJ disc (top view). Reproduced with permission from She Y, Tang S, Zhu Z, *et al.*, *J Biomed Mater Res B Appl Biomater*, 111: 717–29[96]. (D) Schematic representation of the gradient structure of the mandibular condylar fibrocartilage.

4.2. 3D-printed scaffolds for fibrocartilage regeneration

Since the TMJ disc is a fibrocartilage disc containing fibroblasts and chondrocytes, several strategies have been proposed to realize the spatiotemporal delivery of different GFs in the MSCs-loaded 3D-printed scaffolds (Table 2). In 2016, Legemate *et al.*[75] selected CTGF as a pro-fibrogenic factor and TGF-β3 as a chondrogenic factor, both of which were encapsulated with PLGA microspheres (μS). Subsequently, two types of PLGA μS were spatially embedded into 3D-printed PCL scaffolds using EBP to achieve the spatiotemporal delivery of GFs[76]. Fluorescence images showed that TGF-β3 was mainly distributed in the intermediate band of the scaffold, while CTGF was scattered throughout the whole area (Figure 4A and B). Spatiotemporal delivery of GFs led to the formation of inhomogeneous

Table 2. Research on 3D-printed scaffolds for cartilage regeneration in the temporomandibular joint

Reference	3D printing techniques	Study design	Animal model	Cell type	Cell density	Scaffold materials	Bioactive factors
Legemate *et al.* (2016)[75]	EBP	*In vitro*	-	Human BMSCs	2×10^6 cells/mL	PLGA μS + PCL	CTGF, TGF-β3
Tarafder *et al.* (2016)[71]	EBP	*In vitro* and *in vivo*	Rabbit	Human BMSCs	1×10^6 cells/mL	PLGA μS + PCL	CTGF, TGF-β3
Moura *et al.* (2020)[77]	EBP	*In vitro*	-	-	-	PCL + PEGDA	-
Jiang *et al.* (2021)[79]	EBP	*In vitro* and *in vivo*	Goat	Rabbit chondrocytes and fibroblasts	-	(1) PCL + PVA (2) PVA	-
Yi *et al.* (2021)[80]	EBP	*In vitro* and *in vivo*	Mice	Rat costal chondrocytes and L929 fibroblasts	2×10^6 cells/mL	(1) PU-dECM (2) PDA-PU-dECM (3) PCL/PU-dECM (4) PDA-PCL/PU-dECM	-
Ângelo *et al.* (2021)[78]	EBP	*In vivo*	Sheep	-	-	(1) PCL (2) PGS + PCL (3) PCL + PEGDA	-

Abbreviations: EBP, extrusion-based printing; BMSCs, bone mesenchymal stem cells; PEGDA, poly(ethylene glycol) diacrylate; PCL, polycaprolactone; PLGA μS, poly(D,L-lactic-co-glycolic acid) microspheres; PU, polyurethane; dECM, decellularized extracellular matrix; PGS, poly(glycerol sebacate); PDA, polydopamine; CTGF, connective tissue growth factor; TGF-β3, transforming growth factor beta 3; BMP-2, bone morphogenetic protein 2.

fibrocartilaginous tissue in the scaffold after 6 weeks of culture with MSCs (Figure 4C). Furthermore, more collagen and GAG contents were detected in the anterior/posterior bands and the intermediate zone in the scaffolds with a high dose of GFs/μS compared to those with a low dose, while the tensile modulus of the scaffolds was independent of the GF/μS dose. In the same year, Tarafder *et al.*[71] implanted the CTGF/TGF-β3/μS-embedded scaffolds in the intermediate zone and CTGF/μS-embedded scaffolds in the anterior and posterior areas of the perforated rabbit TMJ disc. After 6 weeks *in vivo*, a multi-phase fibrocartilaginous regenerative tissue was observed, and the scaffolds were invisible in the healing TMJ disc. However, the functional properties of the regenerated disc tissue were not tested due to size limitations. Furthermore, the scaffolds with GFs/μS prevented condylar cartilage erosion compared to the scaffolds with empty/μS. These findings suggest the potential application of CTGF/TGF-β3-μS scaffolds in TMJ disc repair.

Recently, novel progress has been made on the modification of PCL-based 3D-printed scaffolds mimicking the TMJ disc (Table 2). To improve the mechanical and morphological properties of PCL-based scaffolds, Moura *et al.*[77] fabricated 3D-printed scaffolds and hydrogels using PCL and poly(ethylene glycol) diacrylate (PEGDA) and investigated the effects of manufacturing parameters and approaches on the product properties (Figure 4D). Compression tests showed that the compression stress and modulus of the PCL-PEGDA multi-material scaffold increased with increasing nozzle temperature (78–86°C). When the filament size was reduced from 300 to 200 μm, the compressive modulus was almost halved. Compared to the PCL scaffold modified with a PEGDA hydrogel shell, the PCL scaffold modified with a PEGDA hydrogel core showed better mechanical properties that were closer to the native disc. In 2021, Ângelo *et al.*[78] further investigated the biological properties of the PCL scaffold with a PEGDA hydrogel shell (PCL +PEGDA) *in vivo*, which was compared to the pure PCL scaffold and poly(glycerol sebacate) (PGS) scaffold modified with electrospun PCL fibers (PGS + PCL). Histologic, imaging, and kinematic analysis demonstrated that no regenerated disc was observed in any group. The PGS + PCL scaffold showed excellent biocompatibility as it was rapidly resorbed. Besides, the PGS + PCL scaffold prevented condylar degenerative changes, which were still observed in both the PCL scaffold and PLA + PEGDA scaffold groups. It is noteworthy that the PCL-based 3D-printed scaffolds in the above-mentioned studies were fabricated without combination seed cells or BFs. Therefore, further research on the effects of seed cells and BFs on the properties of PCL-based 3D-printed scaffolds is needed.

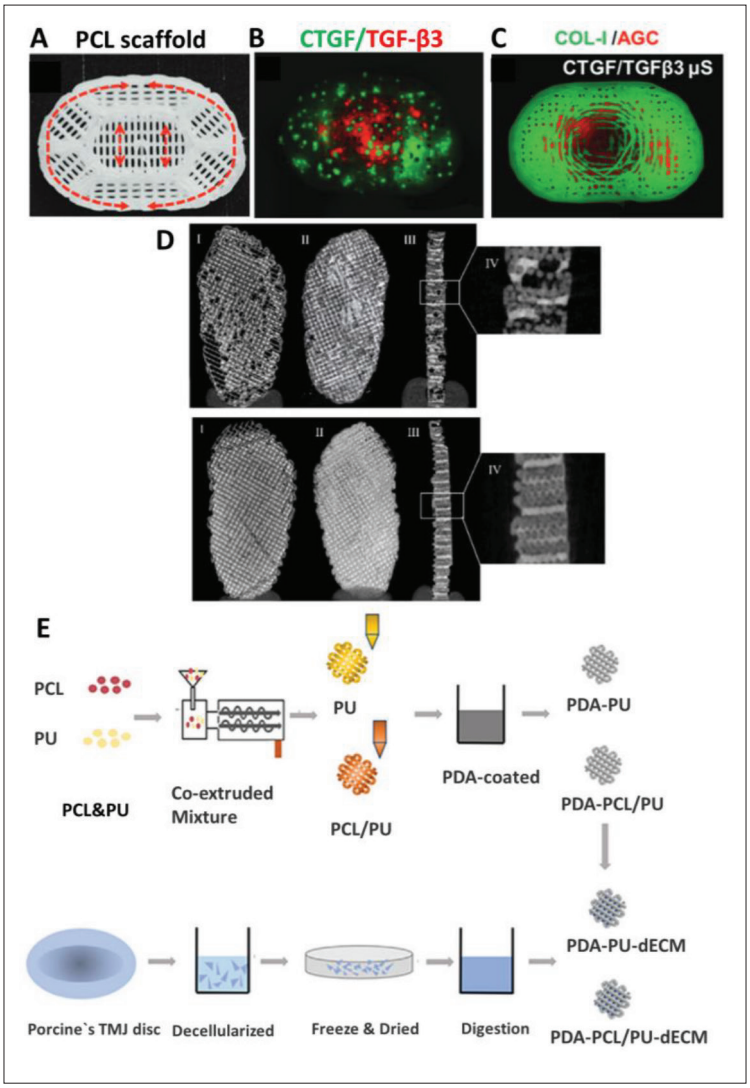

Figure 4. 3D-printed scaffolds for TMJ disc fibrocartilage regeneration. (A) 3D-printed PCL scaffolds of TMJ disc based on the 3D laser scanning data. The size of PCL microstrands (300 μm) and interstrand distance (300 μm) and the relative microstrand density parallel to the alignment direction compared with the perpendicular direction (2:1) were determined to closely approximate the native tensile properties. (B) Spatial control of connective tissue growth factor (CTGF) throughout the scaffolds and transforming growth factor beta 3 (TGF-β3) in the intermediate zone. (C) After a 6-week culture with human mesenchymal stem/progenitor cells, the CTGF and TGF-β3 microsphere-embedded scaffold showed type I collagen throughout the scaffold and aggrecan in the intermediate zone. Reproduced with permission from Legemate K, Tarafder S, Jun Y, *et al*., *J Dent Res*, 95: 800–7[75]. (D) Microcomputed tomography analysis and cross-section images of PCL scaffold modified with a PEGDA shell (upper) and a PEGDA core (lower). (from ref.[77] licensed under Creative Commons Attribution license.) (E) Schematic illustration of the construction process of the composite scaffolds. (from ref.[80] licensed under Creative Commons Attribution license).

Another approach to modify the PCL scaffold is to immerse the 3D-printed PCL scaffold in the PVA hydrogel solution, and network crosslinking is achieved after three freeze-thaw cycles[79]. The *in vitro* study showed that the PVA-PCL scaffold possessed non-cell-adhesive nature, desirable surface smoothness (friction coefficient at 0.0662), similar porosity, compressive property, and viscoelasticity as a natural TMJ disc. The PVA-PCL scaffold was then implanted in the goats to replace the lateral one-third disc. After 3 months, histological analysis showed no degenerative changes in the mandibular condyle, and ingrowth of fibrous tissue was observed around the PCL. A probable explanation was that the gaps between PVA and PCL provided spaces for fibrous tissue ingrowth, which was thought to be an advantage of the PVA-PCL scaffold.

Although the PCL and PU scaffolds usually had smooth surfaces, they lacked the desired ability to promote cell adhesion and growth. To address this challenge, Yi *et al.*[80]

coated the PCL/PU scaffolds with polydopamine (PDA) and then combined them with dECM derived from porcine TMJ discs (Figure 4E). The modified scaffolds exhibited higher tensile modulus and compressive moduli. PDA-PCL/PU and PDA-PU had similar compressive modulus to the central region and the peripheral region of the human TMJ disc, respectively. Compared with the original scaffolds, the chondrogenic-specific markers (*Sox 9* and *Col II*) and fibrous-specific marker (*Col I*) were upregulated in the modified scaffolds after they were seeded with rat costal chondrocytes and L929 fibroblasts and cultured for 14 days. *In vivo* tests further confirmed the ability of the PDA coating to enhance chondrogenesis and fibrogenesis.

5. Mandibular condyle cartilage tissue engineering

5.1. Anatomy

The immunohistochemical staining of the fibrocartilage of the mandibular condyle revealed that type I and type II collagen predominate in the superficial zone and deep zone (the mature and hypertrophic zones), respectively, which is different from articular hyaline cartilage[81]. Specifically, the fibrocartilage covering the upper surface of the mandibular condyle can be subdivided into four layers super-inferiorly: fibrous, proliferating, mature, and hypertrophic zones, where the fiber organization and cellular composition vary (Figure 3D)[82]. Flat-shape fibroblasts and type I collagen occupied the fibrous zone. MSCs, which serve as chondrocyte precursors, were distributed in the proliferative zone. The mature and hypertrophic zones are composed of type II collagen with loose organization and mature chondrocytes. Aggrecan was mainly found in the mature and hypertrophic zones and not in the fibrous zone. The collagen fiber network and proteoglycans provide load-bearing functions to the mandibular condyle. Singh *et al.*[83] divided the mandibular condylar cartilage into three sections in anteroposterior and mediolateral directions, respectively. They discussed the spatial variation of GAGs, anisotropic fiber orientation, and biomechanical properties (compression, tension, and shear) of the condylar cartilage, providing valuable guidance to the fabrication of condylar biomimetic structures with zonal and topographic heterogeneity.

5.2. 3D-printed scaffolds for fibrocartilage regeneration

Several attempts have been reported to achieve mandibular condylar fibrocartilage regeneration *in vivo* using monophasic 3D-printed scaffolds (Table 3). In 2007, Smith *et al.*[84] fabricated PCL scaffolds using selective laser sintering. They filled the condylar head of the scaffold with minipig iliac crest bone marrow and secured the scaffold

Table 3. Research on 3D-printed scaffolds for cartilage regeneration in the mandibular condyle

Reference	3D printing techniques	Study design	Animal model	Cell type	Cell density	Scaffold materials	Bioactive factors
Schek *et al.* (2005)[88]	FDM	*In vivo*	Mice	HGFs	5×10^7 cells/mL	HA	BMP-7
				Pig chondrocytes		PLA	
Smith *et al.* (2007)[84]	SLS	*In vivo*	Minipig	-	-	PCL*	-
Ciocca *et al.* (2013)[87]	SLS	*In vivo*	Sheep	-	-	HA	-
Wang *et al.* (2017)[89]	FDM	*In vitro* and *in vivo*	Mice	Minipig BMSCs	5×10^7 cells/mL	PCL/HA	-
				Minipig chondrocytes	2.5×10^7 cells/mL	PGA/PLA	
Abramowicz *et al.* (2021)[85]	SLS	*In vivo*	Minipig	-	-	PCL	BMP-2
Helgeland *et al.* (2021)[90,91]	EBP	*In vitro*	-	Rat BMSCs	2×10^5 cells/mL; 1.2×10^6 cells/mL	Gelatin**	-

Abbreviations: SLS, selective laser sintering; PCL, polycaprolactone; HA, hydroxyapatite; HGFs, human gingival fibroblasts; FDM, fused deposition modeling; CS, chitosan; PGA/PLA, polyglycolic acid/polylactic acid; BMSCs, bone mesenchymal stem cells; TGF-β1, transforming growth factor beta 1; BMP-2, bone morphogenetic protein 2; PLGA, poly(D, L-lactic-co-glycolic acid); *, the condylar head of the scaffold was packed with iliac crest bone marrow from the minipig; **, the gelatin scaffolds were crosslinked with dehydrothermal, ribose glycation, dehydrothermal-ribose, and genipin, respectively.

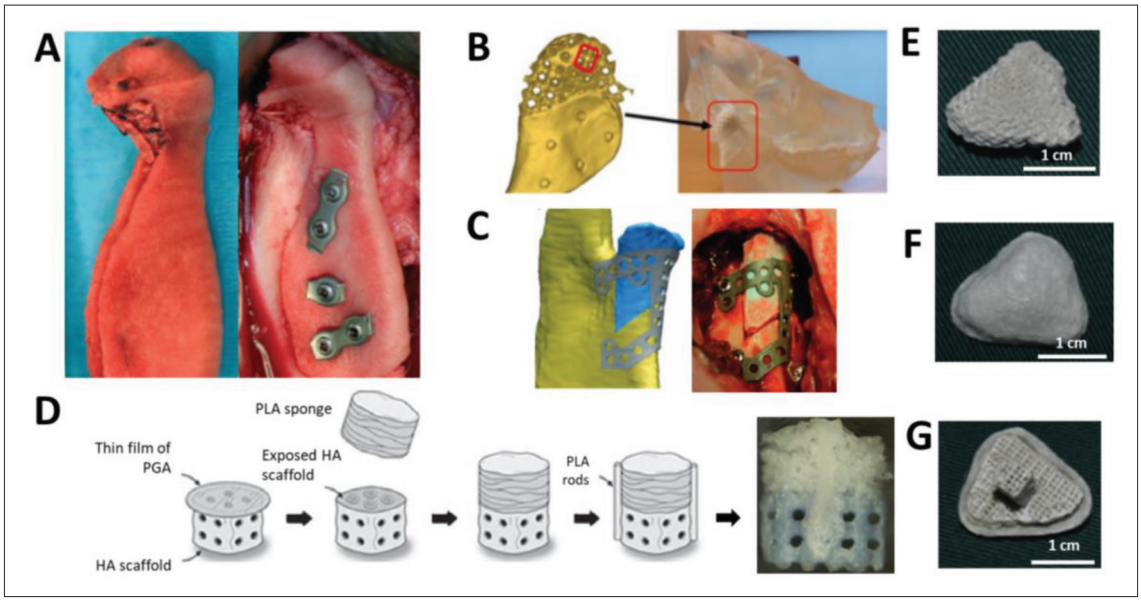

Figure 5. 3D-printed scaffolds for mandibular condylar fibrocartilage regeneration. (A) Iliac crest bone marrow packed into 3D-printed scaffold condylar head (left) and the scaffold well adapted to mandibular ramus (right). Reproduced with permission from Smith MH, Flanagan CL, Kemppainen JM, *et al*., *Int J Med Robot*, 3: 207–16[84]. (B) 3D-printed PCL porous scaffold with collar fixation fit (outlined in red) on 3D-printed pig mandible. Reprinted from *Oral Surg Oral Med Oral Pathol Oral Radiol*, 132: 145–52, Abramowicz S, Crotts SJ, Hollister SJ, Tissue-engineered vascularized patient-specific temporomandibular joint reconstruction in a Yucatan pig model, © (2021), with permission from Elsevier[85]. (C) Visual design (left) and real view (right) of the hydroxyapatite (HA) scaffold and customized bone plates. Reproduced with permission from Ciocca L, Donati D, Fantini M *et al*., *J Biomater Appl*, 28: 207–18[87]. (D) The assembly process and real view of the assembled composite scaffold (upper polymer phase and lower ceramic phase). Reproduced with permission from Schek R, Taboas J, Hollister S, *et al*., *Orthod Craniofac Res*, 8: 313–9[88]. (E–G) The gross images of PCL/HA scaffold (E) and PGA/PLA scaffold (F) and the well-matched biphasic scaffold (G). Reprinted from *J Craniomaxillofac Surg*, 45: 855–61, Wang F, Hu Y, He D, *et al*., Regeneration of subcutaneous tissue-engineered mandibular condyle in nude mice, Copyright 2017, with permission from Elsevier[89].

to the mandibular ramus (Figure 5A). At both the 1- and 3-month time points, the cartilaginous tissue was observed along the articular surface. Nevertheless, the regenerated cartilage was unevenly distributed on the condyle surface and blended with a small amount of bony tissue. Another similar study reported different results. Abramowicz *et al.*[85] found that 6 months after implantation of 3D-printed PCL scaffolds coated with BMP-2 into the mandibular condyle defect, no regenerated cartilage was observed in histologic evaluation (Figure 5B). Although an ideal result for mandibular condylar fibrocartilage regeneration cannot be achieved so far, 3D-printed PCL scaffolds still have great potential in mandibular condylar engineering as they are able to withstand early functional loading due to their mechanical property[86].

Some studies have successfully regenerated both fibrocartilage and the osteochondral interface *in vivo* using either monophasic or biphasic 3D-printed scaffolds (Table 3). In 2013, Ciocca *et al.*[87] fabricated porous HA scaffolds to replace the mandibular condyles in sheep. The HA-F70 (70 vol% total porosity) was selected as the scaffold material as it had the highest compressive strength compared to that of the other three types of HA materials. The customized plates fixed on the bone were used to fix the scaffolds with a single titanium screw (Figure 5C). Four months after surgery, the histological evaluation showed that the regenerated dense fibrocartilage developed on the new articular bone and the osteochondral interface was on average 1.25-mm thick. Notably, several fractures in the material and fragments encapsulated by tissue were observed. Fractures of the scaffold are detrimental to the stability of the scaffold during TMJ movement. In addition, the fixation of the scaffold to the condyle during implantation is of particular concern, as firm primary stability is crucial for osteoblastic and chondroblastic activity.

In 2005, Schek *et al.*[88] fabricated a biphasic PLA/HA scaffold using an image-based design and indirect solid free-form fabrication (Figure 5D). Human gingival fibroblasts transduced with an adenovirus expressing BMP-7 and porcine knee joints chondrocytes were seeded into the lower ceramic phase and the upper polymeric phase, respectively. After subcutaneous implantation into the mice for 4 weeks, the regenerated cartilage, bone, and osteochondral interface were observed in the biphasic scaffold. However, some small pockets of cartilage also occurred within the pores of the ceramic phase, suggesting that greater control of the spatial distribution of the regenerated tissue is required. In 2017, Wang *et al.*[89] further improved the component of the PLA/

HA biphasic scaffold. The PGA/PLA scaffold seeded with chondrocytes and the PCL/HA scaffold seeded with bone MSCs formed a biphasic scaffold (Figure 5E–G). Scanning electron micrographs showed a difference in microscopic structure between the two phases of the scaffold. Twelve weeks after subcutaneous implantation into the dorsum in mice, smooth, continuous, cartilage-like tissue with approximately 1.2-mm thickness covered the surface of the scaffold. Histological examination revealed the regenerated cartilage and the interface between the regenerated cartilage and the subchondral bone. Notably, the auricular chondrocytes seeded in the PGA/PLA scaffold may have been responsible for the reduction of the bone formation in the microchannels of the PCL/HA scaffolds as bone mesenchymal stem cells (BMSCs) have the capacity of biphasic differentiation. Therefore, further research is needed to focus on reducing the effect of chondrocytes (including both auricular and articular chondrocytes) on BMSCs to enhance osteochondral interface formation.

Recent research on 3D-printed gelatin scaffolds has provided new guidance on scaffold fabrication for mandibular condylar engineering. Helgeland *et al.*[90] compared the chemical, mechanical, biological, and physical properties of the 3D-printed gelatin scaffolds crosslinked with dehydrothermal (DHT), ribose glycation, and both. Compared with the DHT-crosslinked and ribose-crosslinked scaffolds, dual-crosslinked scaffolds showed the largest degree of crosslinking, moderate compressive modulus, lowest swelling ratio, highest resistance to hydrolytic and enzymatic degradation, greatest cell proliferation, and lowest expression of the hypertrophy-related collagen 10 gene (*COL10*). In another study by Helgeland *et al.*[91], when 3D-printed gelatin scaffolds were crosslinked by genipin, the stability, swelling, and mechanical properties of gelatin were improved. Unfortunately, the aforementioned improvement in 3D-printed gelatin scaffolds was only demonstrated *in vitro*, so *in vivo* studies are needed to further evaluate the effect of modified 3D-printed gelatin scaffolds.

6. Challenges and prospects

6.1. Current challenges

3D printing is currently at an early stage of development in TMJ tissue engineering, and as such, a large number of challenges remain unresolved, which can be divided into the general cartilage tissue-engineering challenges and the TMJ-specific local challenges.

General challenges faced by 3D-printed scaffolds used for articular cartilage regeneration at different sites include a mismatch between the mechanical properties of the scaffold and the natural cartilage, lack of integration between the scaffold and the natural tissue, and potential immune response induced by the scaffold, etc.[30,92,93] Several recent reviews have discussed potential solutions to these challenges, such as hybrid scaffolds composed of synthetic and natural materials, chemical or non-chemical modification of biomaterials, etc.[30,92,93]

Some additional barriers in TMJ tissue engineering are related to the anatomical structure and location of the TMJ. Although the PCL scaffolds that mimic the organization of the collagen fibers of the TMJ disc have been constructed by 3D printing techniques, the mechanism by which the internal structure of the PCL scaffold regulates cellular behavior and regenerates articular disc tissue remained unclear. The internal structure of the scaffolds has been demonstrated to affect the mechanical stability of the PCL scaffold *in vitro*, and therefore, further *in vivo* studies are needed[65]. In addition, the immunological implications associated with 3D-printed TMJ tissue-engineered products have not been fully investigated in large animal models. Furthermore, given the proximity of the TMJ to the brain, stringent safety guidelines need to be established to facilitate the translation of 3D-printed TMJ tissue-engineered products from research to clinical applications and to reduce the risk of medical accidents[94]. Another challenge is that the existing research on TMJ tissue engineering has employed 3D-printed scaffolds to repair either the TMJ disc or the mandibular condyle only. However, in clinical practice, it is common for osteoarthritis to cause fibrocartilage defects in both the TMJ disc and mandibular condyle at the same time[7]. It is therefore necessary to establish animal models (e.g., goats, minipigs) with articular defects in both the TMJ disc and mandibular condyle, based on which the synergistic effects of the 3D-printed scaffolds used to repair the TMJ disc and mandibular condyle need to be investigated.

6.2. Critical need for support and guidance in TMJ tissue engineering

Partly due to the lack of financial and academic support for TMJ tissue engineering, attempts to promote TMJ fibrocartilage regeneration using 3D-printed scaffolds have been relatively limited so far. There is a large gap between knee and TMJ tissue engineering in terms of research funding, academic publications, and research translation, despite similarities in the incidence of knee and TMJ osteoarthritis[95]. There is a lack of sufficient primary research in TMJ tissue engineering, resulting in a paucity of TMJ tissue-engineered products and human clinical trials. The limited number of human clinical trials results in the low availability of marketed TMJ products and little to no commercial support for TMJ products. This exacerbates the lack of industrial guidance and research funding for the

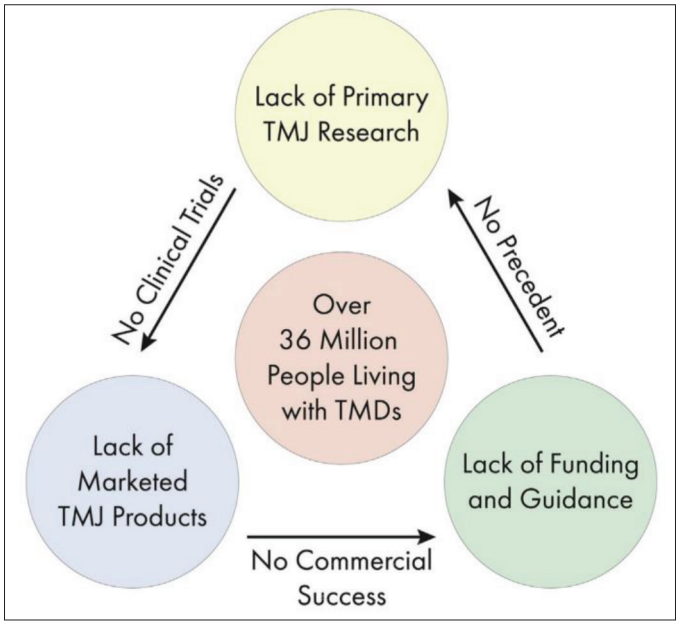

Figure 6. The vicious cycle of TMJ translational research. (from ref.[95] licensed under Creative Commons Attribution 4.0 license).

TMJ tissue engineering, resulting in a vicious cycle of TMJ translational research (Figure 6). Considering knee tissue engineering as an important reference, several approaches and suggestions have been raised to promote TMJ tissue engineering, such as increasing the amount of rigorous TMJ research, strengthening surgical training opportunities and research grants for TMJ physicians and researchers, holding large-scale interdisciplinary conferences on TMJ, establishing clear indications and industry guidance for TMJ tissue-engineered products, and so on[95]. On the other hand, the anatomical structures, functions, and biomechanical properties of the TMJ disc, meniscus, and intervertebral disc have been compared in a recent review, suggesting that their similarities may guide the imitation and improvement of TMJ tissue-engineered products in seed cells, scaffold materials, and BFs[96]. In general, there is an urgent need for increased interdisciplinary collaboration, societal support, and financial investment in TMJ tissue engineering.

6.3. Emerging tissue-engineering strategies

3D printing technology has provided new impetus for the development of TMJ fibrocartilage tissue engineering, but satisfactory results have rarely been achieved so far. Several tissue-engineering strategies are considered potential approaches to improve the performance of 3D-printed TMJ scaffolds and are therefore briefly presented below (Figure 7).

To better regulate the complex effects of printing parameters on the quality of 3D-printed products, machine learning (ML) has been introduced to the biomaterials field as a promising approach to quantitatively assess printability and optimize printing parameters[97]. Recently, Conev *et al.*[98] predicted the quality of 3D-printed products from the material composition and printing parameters using an ML model. Similar work was done by Ruberu *et al.*[99], who adopted ML to create the optimal printing parameters protocol, including ink composition, ink reservoir temperature, driving pressure, needle speed, and platform temperature. Furthermore, the effect of nozzle geometry, printing pressure, and material properties on cell viability was analyzed by Reina-Romo *et al.*[100] using an ML approach named Gaussian Process. ML shows great potential as a novel approach to improve the biological properties of 3D-printed scaffolds.

Although BFs play an important role in TMJ fibrocartilage regeneration, they are rarely used, mainly due to the lack of an effective approach to realize spatiotemporally controlled release of BFs. As mentioned in the previous studies, microspheres loading BFs have been demonstrated to possess the ability to realize spatially-controlled delivery of BFs with a prolonged release[71,75]. However, the release of BFs from microspheres remains passive and unable to interact with the local biological microenvironment[71,75]. Stimuli-responsive delivery systems for growth factors may be the solution to the developmental asynchrony of different components of the heterogeneous TMJ tissues in the regeneration process. The release of stimuli-responsive delivery systems can be triggered by, for example, a specific pH, biomolecule recognition, and external stimuli, such as temperature, ultrasound, magnetic, voltage, and light[101,102]. For example, the release of BMP-7 and BMP-2 at different times and sequences using light-triggered delivery systems is regulated by different wavelengths of light[103].

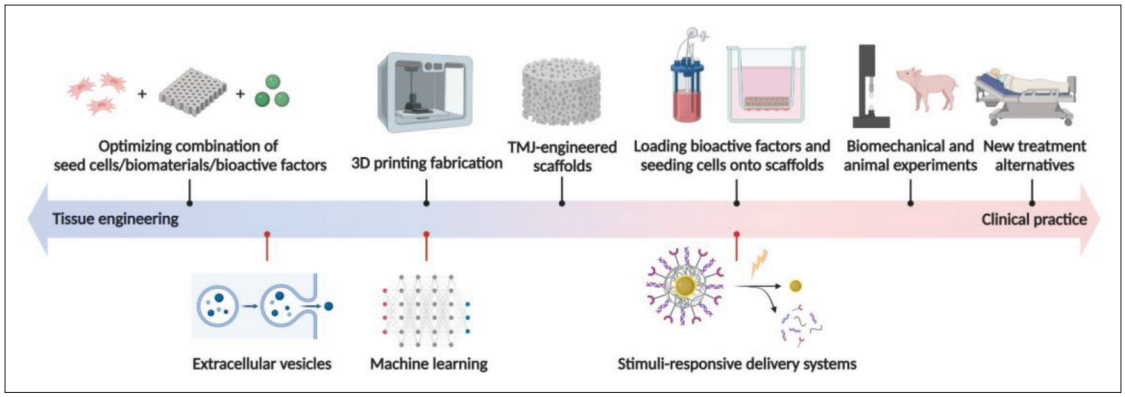

Figure 7. Schematic illustration of some emerging tissue-engineering strategies (lower row) potentially promoting the research translation (upper row) of TMJ fibrocartilage tissue engineering.

Extracellular vesicles (EVs) containing various paracrine signaling agents are another approach to deliver BFs to the tissue defect. MSC-derived EVs have been reported to induce progenitor cells migration, facilitate cartilage and bone regeneration, and relieve pain in TMJ osteoarthritis animal models[63]. Chen *et al.*[104] further demonstrated that the 3D-printed scaffolds loaded with MSC-derived EVs facilitated the regeneration of osteochondral defects using a rabbit model, providing an ideal example of the combination of 3D printing techniques and EVs in cartilage tissue engineering. Several recent reviews have provided new perspectives for the adoption of EVs as promising engineered product components to promote fibrocartilage regeneration for TMJ osteoarthritis patients[105-107].

With the advancement of regenerative medicine, 3D printing techniques have shown great ability to fabricate complex bionic products to promote the regeneration of various tissues. Although TMJ tissue engineering remains an evolving field with many challenges to date, the continued attempts to combine 3D printing techniques with TMJ tissue engineering will likely bring us closer to a future where 3D-printed tissue-engineered products become an effective treatment for TMJ osteoarthritis in clinical practice.

Acknowledgments

None.

Funding

This research was supported by National Natural Science Foundation of China (No. 82101059) to Y.Y.; National Natural Science Foundation of China (No. 81970967, 82271019), Sichuan Health Commission Medical Science and Technology Program (21ZD003), and Research and Develop Program, West China Hospital of Stomatology Sichuan University (RD-03-202101) to J.W.

Conflict of interest

The authors declare no potential conflicts of interest concerning the research, authorship, and/or publication of this article.

Author contributions

Conceptualization: Shoushan Hu, Yating Yi
Funding acquisition: Yating Yi, Jun Wang
Project administration: Jin Liu, Jun Wang
Visualization: Shoushan Hu, Chengxinyue Ye
Writing – original draft: Shoushan Hu, Yating Yi
Writing – review & editing: All authors

Ethics approval and consent to participate

Not applicable.

Consent for publication

Not applicable.

Availability of data

Not applicable.

References

1. Alomar X, Medrano J, Cabratosa J, *et al.*, 2007, Anatomy of the temporomandibular joint. *Semin Ultrasound CT MR*, 28(3): 170–183.

http://doi.org/10.1053/j.sult.2007.02.002

2. de Souza RF, Lovato da Silva CH, Nasser M, *et al.*, 2012, Interventions for the management of temporomandibular joint osteoarthritis. *Cochrane Database Syst Rev*, 2012(4): Cd007261.

http://doi.org/10.1002/14651858.CD007261.pub2

3. Valesan LF, Da-Cas CD, Réus JC, *et al.*, 2021, Prevalence of temporomandibular joint disorders: A systematic review and meta-analysis. *Clin Oral Investig*, 25(2): 441–53

http://doi.org/10.1007/s00784-020-03710-w

4. Tanaka E, Detamore MS, Mercuri LG, 2008, Degenerative disorders of the temporomandibular joint: Etiology, diagnosis, and treatment. *J Dent Res*, 87(4): 296–307

http://doi.org/10.1177/154405910808700406

5. Fang L, Ye Y, Tan X, *et al.*, 2021, Overloading stress-induced progressive degeneration and self-repair in condylar cartilage. *Ann N Y Acad Sci*, 1503(1): 72–87

http://doi.org/10.1111/nyas.14606

6. Lee KS, Kwak HJ, Oh JM, *et al.*, 2020, Automated detection of TMJ osteoarthritis based on artificial intelligence. *J Dent Res*, 99(12): 1363–7

http://doi.org/10.1177/0022034520936950

7. Wang XD, Zhang JN, Gan YH, *et al.*, 2015, Current understanding of pathogenesis and treatment of TMJ osteoarthritis. *J Dent Res*, 94(5): 666–73

http://doi.org/10.1177/0022034515574770

8. Resnick CM, 2018, Temporomandibular joint reconstruction in the growing child. *Oral Maxillofac Surg Clin North Am*, 30(1): 109–21

http://doi.org/10.1016/j.coms.2017.08.006

9. Haene R, Qamirani E, Story RA, *et al.*, 2012, Intermediate outcomes of fresh talar osteochondral allografts for treatment of large osteochondral lesions of the talus. *J Bone Joint Surg Am*, 94(12): 1105–10

http://doi.org/10.2106/jbjs.J.02010

10. Johnson NR, Roberts MJ, Doi SA, *et al.*, 2017, Total temporomandibular joint replacement prostheses: A systematic review and bias-adjusted meta-analysis. *Int J Oral Maxillofac Surg*, 46(1): 86–92

http://doi.org/10.1016/j.ijom.2016.08.022

11. Armiento AR, Stoddart MJ, Alini M, *et al.*, 2018, Biomaterials for articular cartilage tissue engineering: Learning from biology. *Acta Biomater*, 65: 1–20.

http://doi.org/10.1016/j.actbio.2017.11.021

12. O'Shea DG, Curtin CM, O'Brien FJ, 2022, Articulation inspired by nature: A review of biomimetic and biologically active 3D printed scaffolds for cartilage tissue engineering. *Biomater Sci*, 10(10): 2462–83.

http://doi.org/10.1039/d1bm01540k

13. Van Bellinghen X, Idoux-Gillet Y, Pugliano M, *et al.*, 2018, Temporomandibular joint regenerative medicine. *Int J Mol Sci*, 19(2): 446.

http://doi.org/10.3390/ijms19020446

14. Trindade D, Cordeiro R, José HC, *et al.*, 2021, Biological treatments for temporomandibular joint disc disorders: Strategies in tissue engineering. *Biomolecules*, 11(7): 933.

http://doi.org/10.3390/biom11070933

15. Perera K, Ivone R, Natekin E, *et al.*, 2021, 3D bioprinted implants for cartilage repair in intervertebral discs and knee menisci. *Front Bioeng Biotechnol*, 9: 754113.

http://doi.org/10.3389/fbioe.2021.754113

16. Doyle SE, Snow F, Duchi S, *et al.*, 2021, 3D printed multiphasic scaffolds for osteochondral repair: Challenges and opportunities. *Int J Mol Sci*, 22(22): 12420.

http://doi.org/10.3390/ijms222212420

17. Wang S, Zhao S, Yu J, *et al.*, 2022, Advances in translational 3D printing for cartilage, bone, and osteochondral tissue engineering. *Small*, 18(36): e2201869.

http://doi.org/10.1002/smll.202201869

18. McMillan A, McMillan N, Gupta N, *et al.*, 2023, 3D bioprinting in otolaryngology: A review. *Adv Healthc Mater*, e2203268.

http://doi.org/10.1002/adhm.202203268

19. Yang Z, Yi P, Liu Z, *et al.*, 2022, Stem cell-laden hydrogel-based 3D bioprinting for bone and cartilage tissue engineering. *Front Bioeng Biotechnol*, 10: 865770.

http://doi.org/10.3389/fbioe.2022.865770

20. Zub K, Hoeppener S, Schubert US, 2022, Inkjet printing and 3D printing strategies for biosensing, analytical, and diagnostic applications. *Adv Mater*, 34(31): e2105015.

http://doi.org/10.1002/adma.202105015

21. Gudapati H, Dey M, Ozbolat I, 2016, A comprehensive review on droplet-based bioprinting: Past, present and future. *Biomaterials*, 102: 20–42.

http://doi.org/10.1016/j.biomaterials.2016.06.012

22. Sohrabi S, Liu Y, 2018, Modeling thermal inkjet and cell printing process using modified pseudopotential and thermal lattice Boltzmann methods. *Phys Rev E*, 97(3–1): 033105.

http://doi.org/10.1103/PhysRevE.97.033105

23. Mandrycky C, Wang Z, Kim K, *et al.*, 2016, 3D bioprinting for engineering complex tissues. *Biotechnol Adv*, 34(4): 422–34.

http://doi.org/10.1016/j.biotechadv.2015.12.011

24. Guo Q, Su X, Zhang X, *et al.*, 2021, A review on acoustic droplet ejection technology and system. *Soft Matter*, 17(11): 3010–21.

http://doi.org/10.1039/d0sm02193h

25. Derakhshanfar S, Mbeleck R, Xu K, *et al.*, 2018, 3D bioprinting for biomedical devices and tissue engineering: A review of recent trends and advances. *Bioact Mater*, 3(2): 144–56.

http://doi.org/10.1016/j.bioactmat.2017.11.008

26. Zhang YS, Haghiashtiani G, Hübscher T, *et al.*, 2021, 3D extrusion bioprinting. *Nat Rev Methods Primers*, 1(1): 75.

    http://doi.org/10.1038/s43586-021-00073-8

27. Liu H, Zhou H, Lan H, *et al.*, 2018, Multinozzle multichannel temperature deposition system for construction of a blood vessel. *SLAS Technol*, 23(1): 64–9.

    http://doi.org/10.1177/2472630317712221

28. Hong S, Kim JS, Jung B, *et al.*, 2019, Coaxial bioprinting of cell-laden vascular constructs using a gelatin-tyramine bioink. *Biomater Sci*, 7(11): 4578–87.

    http://doi.org/10.1039/c8bm00618k

29. Daly AC, Freeman FE, Gonzalez-Fernandez T, *et al.*, 2017, 3D bioprinting for cartilage and osteochondral tissue engineering. *Adv Healthc Mater*, 6(22): 1700298.

    http://doi.org/10.1002/adhm.201700298

30. Li M, Sun D, Zhang J, *et al.*, 2022, Application and development of 3D bioprinting in cartilage tissue engineering. *Biomater Sci*, 10(19):5430–58.

    http://doi.org/10.1039/d2bm00709f

31. Ozbolat IT, Hospodiuk M, 2016, Current advances and future perspectives in extrusion-based bioprinting. *Biomaterials*, 76: 321–43.

    http://doi.org/10.1016/j.biomaterials.2015.10.076

32. Heinrich MA, Liu W, Jimenez A, *et al.*, 2019, 3D bioprinting: From benches to translational applications. *Small*, 15(23): e1805510.

    http://doi.org/10.1002/smll.201805510

33. Kačarević ŽP, Rider PM, Alkildani S, *et al.*, 2018, An introduction to 3D bioprinting: Possibilities, challenges and future aspects. *Materials (Basel)*, 11(11): 2199.

    http://doi.org/10.3390/ma11112199

34. Bohandy JB, Kim BF, Adrian FJ, 1986, Metal deposition from a supported metal film using an excimer laser. *J Appl Phys*, 60(4): 1538–9.

    http://doi.org/10.1063/1.337287

35. Li J, Chen M, Fan X, *et al.*, 2016, Recent advances in bioprinting techniques: Approaches, applications and future prospects. *J Transl Med*, 14: 271.

    http://doi.org/10.1186/s12967-016-1028-0

36. Catros S, Guillotin B, BacÁková M, *et al.*, 2011, Effect of laser energy, substrate film thickness and bioink viscosity on viability of endothelial cells printed by laser-assisted bioprinting. *Appl Surf Sci*, 257(12): 5142–7.

    http://doi.org/10.1016/j.apsusc.2010.11.049

37. Su X, Wang T, Guo S, 2021, Applications of 3D printed bone tissue engineering scaffolds in the stem cell field. *Regen Ther*, 16: 63–72.

    http://doi.org/10.1016/j.reth.2021.01.007

38. Zhang J, Hu Q, Wang S, *et al.*, 2020, Digital light processing based three-dimensional printing for medical applications. *Int J Bioprint*, 6(1): 242.

    http://doi.org/10.18063/ijb.v6i1.242

39. Wu Y, Su H, Li M, *et al.*, 2022, Digital light processing-based multi-material bioprinting: Processes, applications, and perspectives. *J Biomed Mater Res A*, 111(4): 527–42.

    http://doi.org/10.1002/jbm.a.37473

40. Kadry H, Wadnap S, Xu C, *et al.*, 2019, Digital light processing (DLP) 3D-printing technology and photoreactive polymers in fabrication of modified-release tablets. *Eur J Pharm Sci*, 135: 60–7.

    http://doi.org/10.1016/j.ejps.2019.05.008

41. Ravanbakhsh H, Karamzadeh V, Bao G, *et al.*, 2021, Emerging technologies in multi-material bioprinting. *Adv Mater*, 33(49): e2104730.

    http://doi.org/10.1002/adma.202104730

42. Godbey WT, Hindy SB, Sherman ME, *et al.*, 2004, A novel use of centrifugal force for cell seeding into porous scaffolds. *Biomaterials*, 25(14): 2799–2805.

    http://doi.org/10.1016/j.biomaterials.2003.09.056

43. Griffon DJ, Abulencia JP, Ragetly GR, *et al.*, 2011, A comparative study of seeding techniques and three-dimensional matrices for mesenchymal cell attachment. *J Tissue Eng Regen Med*, 5(3): 169–179.

    http://doi.org/10.1002/term.302

44. Collon K, Bell JA, Chang SW, *et al.*, 2022, Effects of cell seeding technique and cell density on BMP-2 production in transduced human mesenchymal stem cells. *J Biomed Mater Res A*, 110(12): 1944–1952.

    http://doi.org/10.1002/jbm.a.37430

45. Anderson DE, Athanasiou KA, 2009, A comparison of primary and passaged chondrocytes for use in engineering the temporomandibular joint. *Arch Oral Biol*, 54(2): 138–145.

    http://doi.org/10.1016/j.archoralbio.2008.09.018

46. Anderson DE, Athanasiou KA, 2008, Passaged goat costal chondrocytes provide a feasible cell source for temporomandibular joint tissue engineering. *Ann Biomed Eng*, 36(12): 1992–2001.

    http://doi.org/10.1007/s10439-008-9572-2

47. Vapniarsky N, Huwe LW, Arzi B, *et al.*, 2018, Tissue engineering toward temporomandibular joint disc regeneration. *Sci Transl Med*, 10(446): eaaq1802.

    http://doi.org/10.1126/scitranslmed.aaq1802

48. Kalpakci KN, Kim EJ, Athanasiou KA, 2011, Assessment of growth factor treatment on fibrochondrocyte and chondrocyte co-cultures for TMJ fibrocartilage engineering. *Acta Biomater*, 7(4): 1710–1718.

    http://doi.org/10.1016/j.actbio.2010.12.015

49. Cui D, Li H, Xu X, *et al.*, 2017, Mesenchymal stem cells for cartilage regeneration of TMJ osteoarthritis. *Stem Cells Int*, 2017: 5979741.

http://doi.org/10.1155/2017/5979741

50. Bousnaki M, Bakopoulou A, Papadogianni D, *et al.*, 2018, Fibro/chondrogenic differentiation of dental stem cells into chitosan/alginate scaffolds towards temporomandibular joint disc regeneration. *J Mater Sci Mater Med*, 29(7): 97.

http://doi.org/10.1007/s10856-018-6109-6

51. Park YB, Ha CW, Lee CH, *et al.*, 2017, Restoration of a large osteochondral defect of the knee using a composite of umbilical cord blood-derived mesenchymal stem cells and hyaluronic acid hydrogel: A case report with a 5-year follow-up. *BMC Musculoskelet Disord*, 18(1): 59.

http://doi.org/10.1186/s12891-017-1422-7

52. Liu J, Nie H, Xu Z, *et al.*, 2014, The effect of 3D nanofibrous scaffolds on the chondrogenesis of induced pluripotent stem cells and their application in restoration of cartilage defects. *PLoS One*, 9(11): e111566.

http://doi.org/10.1371/journal.pone.0111566

53. Zhang J, Guo F, Mi J, *et al.*, 2014, Periodontal ligament mesenchymal stromal cells increase proliferation and glycosaminoglycans formation of temporomandibular joint derived fibrochondrocytes. *Biomed Res Int*, 2014: 410167.

http://doi.org/10.1155/2014/410167

54. Ogasawara N, Kano F, Hashimoto N, *et al.*, 2020, Factors secreted from dental pulp stem cells show multifaceted benefits for treating experimental temporomandibular joint osteoarthritis. *Osteoarthr Cartil*, 28(6): 831–841.

http://doi.org/10.1016/j.joca.2020.03.010

55. Sun AX, Lin H, Fritch MR, *et al.*, 2017, Chondrogenesis of human bone marrow mesenchymal stem cells in 3-dimensional, photocrosslinked hydrogel constructs: Effect of cell seeding density and material stiffness. *Acta Biomater*, 58: 302–311.

http://doi.org/10.1016/j.actbio.2017.06.016

56. Sophia Fox AJ, Bedi A, Rodeo SA, 2009, The basic science of articular cartilage: Structure, composition, and function. *Sports Health*, 1(6): 461–468.

http://doi.org/10.1177/1941738109350438

57. Hunziker EB, Quinn TM, Häuselmann HJ, 2002, Quantitative structural organization of normal adult human articular cartilage. *Osteoarthr Cartil*, 10(7): 564–572.

http://doi.org/10.1053/joca.2002.0814

58. Ren X, Wang F, Chen C, *et al.*, 2016, Engineering zonal cartilage through bioprinting collagen type II hydrogel constructs with biomimetic chondrocyte density gradient. *BMC Musculoskelet Disord*, 17: 301.

http://doi.org/10.1186/s12891-016-1130-8

59. Talukdar S, Nguyen QT, Chen AC, *et al.*, 2011, Effect of initial cell seeding density on 3D-engineered silk fibroin scaffolds for articular cartilage tissue engineering. *Biomaterials*, 32(34): 8927–8937.

http://doi.org/10.1016/j.biomaterials.2011.08.027

60. Lam T, Dehne T, Krüger JP, *et al.*, 2019, Photopolymerizable gelatin and hyaluronic acid for stereolithographic 3D bioprinting of tissue-engineered cartilage. *J Biomed Mater Res B Appl Biomater*, 107(8): 2649–2657.

http://doi.org/10.1002/jbm.b.34354

61. Li X, Teng Y, Liu J, *et al.*, 2017, Chondrogenic differentiation of BMSCs encapsulated in chondroinductive polysaccharide/collagen hybrid hydrogels. *J Mater Chem B*, 5(26): 5109–5119.

http://doi.org/10.1039/c7tb01020f

62. Kim M, Erickson IE, Huang AH, *et al.*, 2018, Donor variation and optimization of human mesenchymal stem cell chondrogenesis in hyaluronic acid. *Tissue Eng Part A*, 24(21-22): 1693–1703.

http://doi.org/10.1089/ten.TEA.2017.0520

63. Wang D, Qi Y, Wang Z, *et al.*, 2022, Recent advances in animal models, diagnosis, and treatment of temporomandibular joint osteoarthritis. *Tissue Eng Part B Rev*, 29(1): 62–77.

http://doi.org/10.1089/ten.TEB.2022.0065

64. Yang X, Lu Z, Wu H, *et al.*, 2018, Collagen-alginate as bioink for three-dimensional (3D) cell printing based cartilage tissue engineering. *Mater Sci Eng C Mater Biol Appl*, 83: 195–201.

http://doi.org/10.1016/j.msec.2017.09.002

65. Huber F, Vollmer D, Vinke J, *et al.*, 2022, Influence of 3D printing parameters on the mechanical stability of PCL scaffolds and the proliferation behavior of bone cells. *Materials (Basel)*, 15(6): 2091.

http://doi.org/10.3390/ma15062091

66. Lu J, Huang J, Jin J, *et al.*, 2022, The design and characterization of a strong bio-ink for meniscus regeneration. *Int J Bioprint*, 8(4): 600.

http://doi.org/10.18063/ijb.v8i4.600

67. Li P, Fu L, Liao Z, *et al.*, 2021, Chitosan hydrogel/3D-printed poly(ε-caprolactone) hybrid scaffold containing synovial mesenchymal stem cells for cartilage regeneration based on tetrahedral framework nucleic acid recruitment. *Biomaterials*, 278: 121131.

http://doi.org/10.1016/j.biomaterials.2021.121131

68. Shen H, Hu X, 2021, Growth factor loading on aliphatic polyester scaffolds. *RSC Adv*, 11(12): 6735–6747.

http://doi.org/10.1039/d0ra10232f

69. Acri TM, Shin K, Seol D, *et al.*, 2019, Tissue engineering for the temporomandibular joint. *Adv Healthc Mater*, 8(2): e1801236.

http://doi.org/10.1002/adhm.201801236

70. Luo C, Xie R, Zhang J, *et al.*, 2020, Low-temperature three-dimensional printing of tissue cartilage engineered with gelatin methacrylamide. *Tissue Eng Part C Methods*, 26(6): 306–316.

http://doi.org/10.1089/ten.TEC.2020.0053

71. Tarafder S, Koch A, Jun Y, *et al.*, 2016, Micro-precise spatiotemporal delivery system embedded in 3D printing for complex tissue regeneration. *Biofabrication*, 8(2): 025003.

http://doi.org/10.1088/1758-5090/8/2/025003

72. Dormer NH, Busaidy K, Berkland CJ, *et al.*, 2011, Osteochondral interface regeneration of rabbit mandibular condyle with bioactive signal gradients. *J Oral Maxillofac Surg*, 69(6): e50–57.

http://doi.org/10.1016/j.joms.2010.12.049

73. Kalpakci KN, Willard VP, Wong ME, *et al.*, 2011, An interspecies comparison of the temporomandibular joint disc. *J Dent Res*, 90(2): 193–198.

http://doi.org/10.1177/0022034510381501

74. Kuo J, Zhang L, Bacro T, *et al.*, 2010, The region-dependent biphasic viscoelastic properties of human temporomandibular joint discs under confined compression. *J Biomech*, 43(7): 1316–1321.

http://doi.org/10.1016/j.jbiomech.2010.01.020

75. Legemate K, Tarafder S, Jun Y, *et al.*, 2016, Engineering human TMJ discs with protein-releasing 3D-printed scaffolds. *J Dent Res*, 95(7): 800–807.

http://doi.org/10.1177/0022034516642404

76. Lee CH, Rodeo SA, Fortier LA, *et al.*, 2014, Protein-releasing polymeric scaffolds induce fibrochondrocytic differentiation of endogenous cells for knee meniscus regeneration in sheep. *Sci Transl Med*, 6(266): 266ra171.

http://doi.org/10.1126/scitranslmed.3009696

77. Moura C, Trindade D, Vieira M, *et al.*, 2020, Multi-material implants for temporomandibular joint disc repair: Tailored additive manufacturing production. *Front Bioeng Biotechnol*, 8: 342.

http://doi.org/10.3389/fbioe.2020.00342

78. Ângelo DF, Wang Y, Morouço P, *et al.*, 2021, A randomized controlled preclinical trial on 3 interposal temporomandibular joint disc implants: TEMPOJIMS-Phase 2. *J Tissue Eng Regen Med*, 15(10): 852–868.

http://doi.org/10.1002/term.3230

79. Jiang N, Yang Y, Zhang L, *et al.*, 2021, 3D-printed polycaprolactone reinforced hydrogel as an artificial TMJ disc. *J Dent Res*, 100(8): 839–846.

http://doi.org/10.1177/00220345211000629

80. Yi P, Liang J, Huang F, *et al.*, 2021, Composite system of 3D-printed polymer and acellular matrix hydrogel to repair temporomandibular joint disc. *Front Mater*, 8: 621416.

http://doi.org/10.3389/fmats.2021.621416

81. Wang L, Lazebnik M, Detamore MS, 2009, Hyaline cartilage cells outperform mandibular condylar cartilage cells in a TMJ fibrocartilage tissue engineering application. *Osteoarthr Cartil*, 17(3): 346–353.

http://doi.org/10.1016/j.joca.2008.07.004

82. Stocum DL, Roberts WE, 2018, Part I: Development and physiology of the temporomandibular joint. *Curr Osteoporos Rep*, 16(4): 360–368.

http://doi.org/10.1007/s11914-018-0447-7

83. Singh M, Detamore MS, 2009, Biomechanical properties of the mandibular condylar cartilage and their relevance to the TMJ disc. *J Biomech*, 42(4): 405–417.

http://doi.org/10.1016/j.jbiomech.2008.12.012

84. Smith MH, Flanagan CL, Kemppainen JM, *et al.*, 2007, Computed tomography-based tissue-engineered scaffolds in craniomaxillofacial surgery. *Int J Med Robot*, 3(3): 207–216.

http://doi.org/10.1002/rcs.143

85. Abramowicz S, Crotts SJ, Hollister SJ, *et al.*, 2021, Tissue-engineered vascularized patient-specific temporomandibular joint reconstruction in a Yucatan pig model. *Oral Surg Oral Med Oral Pathol Oral Radiol*, 132(2): 145–152.

http://doi.org/10.1016/j.oooo.2021.02.002

86. Williams JM, Adewunmi A, Schek RM, *et al.*, 2005, Bone tissue engineering using polycaprolactone scaffolds fabricated via selective laser sintering. *Biomaterials*, 26(23): 4817–4827.

http://doi.org/10.1016/j.biomaterials.2004.11.057

87. Ciocca L, Donati D, Fantini M, *et al.*, 2013, CAD-CAM-generated hydroxyapatite scaffold to replace the mandibular condyle in sheep: Preliminary results. *J Biomater Appl*, 28(2): 207–218.

http://doi.org/10.1177/0885328212443296

88. Schek R, Taboas J, Hollister S, *et al.*, 2005, Tissue engineering osteochondral implants for temporomandibular joint repair. *Orthod Craniofac Res*, 8(4): 313–319.

http://doi.org/https://doi.org/10.1111/j.1601-6343.2005.00354.x

89. Wang F, Hu Y, He D, *et al.*, 2017, Regeneration of subcutaneous tissue-engineered mandibular condyle in nude mice. *J Craniomaxillofac Surg*, 45(6): 855–861.

http://doi.org/10.1016/j.jcms.2017.03.017

90. Helgeland E, Rashad A, Campodoni E, *et al.*, 2021, Dual-crosslinked 3D printed gelatin scaffolds with potential for temporomandibular joint cartilage regeneration. *Biomed Mater*, 16(3): 035026.

http://doi.org/10.1088/1748-605X/abe6d9

91. Helgeland E, Mohamed-Ahmed S, Shanbhag S, *et al.*, 2021, 3D printed gelatin-genipin scaffolds for temporomandibular

joint cartilage regeneration. *Biomed Phys Eng Express*, 7(5): 055025.

http://doi.org/10.1088/2057-1976/ac1e68

92. Donahue RP, Hu JC, Athanasiou KA, 2019, Remaining hurdles for tissue-engineering the temporomandibular joint disc. *Trends Mol Med*, 25(3): 241–256.

http://doi.org/10.1016/j.molmed.2018.12.007

93. Murphy SV, De Coppi P, Atala A, 2020, Opportunities and challenges of translational 3D bioprinting. *Nat Biomed Eng*, 4(4): 370–380.

http://doi.org/10.1038/s41551-019-0471-7

94. Chuong R, Piper MA, 1992, Cerebrospinal fluid leak associated with proplast implant removal from the temporomandibular joint. *Oral Surg Oral Med Oral Pathol*, 74(4): 422–425.

http://doi.org/10.1016/0030-4220(92)90286-y

95. Bielajew BJ, Donahue RP, Espinosa MG, *et al.*, 2021, Knee orthopedics as a template for the temporomandibular joint. *Cell Rep Med*, 2(5): 100241.

http://doi.org/10.1016/j.xcrm.2021.100241

96. She Y, Tang S, Zhu Z, *et al.*, 2022, Comparison of temporomandibular joint disc, meniscus, and intervertebral disc in fundamental characteristics and tissue engineering. *J Biomed Mater Res B Appl Biomater*, 111(3): 717–729.

http://doi.org/10.1002/jbm.b.35178

97. Malekpour A, Chen X, 2022, Printability and cell viability in extrusion-based bioprinting from experimental, computational, and machine learning views. *J Funct Biomater*, 13(2): 40.

http://doi.org/10.3390/jfb13020040

98. Conev A, Litsa EE, Perez MR, *et al.*, 2020, Machine learning-guided three-dimensional printing of tissue engineering scaffolds. *Tissue Eng Part A*, 26(23–24): 1359–1368.

http://doi.org/10.1089/ten.TEA.2020.0191

99. Ruberu K, Senadeera M, Rana S, *et al.*, 2021, Coupling machine learning with 3D bioprinting to fast track optimisation of extrusion printing. *Appl Mater Today*, 22: 100914.

http://doi.org/10.1016/j.apmt.2020.100914

100. Reina-Romo E, Mandal S, Amorim P, *et al.*, 2021, Towards the experimentally-informed in silico nozzle design optimization for extrusion-based bioprinting of shear-thinning hydrogels. *Front Bioeng Biotechnol*, 9: 701778.

http://doi.org/10.3389/fbioe.2021.701778

101. Caballero Aguilar LM, Silva SM, Moulton SE, 2019, Growth factor delivery: Defining the next generation platforms for tissue engineering. *J Control Release*, 306: 40–58.

http://doi.org/10.1016/j.jconrel.2019.05.028

102. Zhang M, Hu W, Cai C, *et al.*, 2022, Advanced application of stimuli-responsive drug delivery system for inflammatory arthritis treatment. *Materials Today Bio*, 14: 100223.

http://doi.org/10.1016/j.mtbio.2022.100223

103. Azagarsamy MA, Anseth KS, 2013, Wavelength-controlled photocleavage for the orthogonal and sequential release of multiple proteins. *Angew Chem Int Ed Engl*, 52(51): 13803–13807.

http://doi.org/10.1002/anie.201308174

104. Chen P, Zheng L, Wang Y, *et al.*, 2019, Desktop-stereolithography 3D printing of a radially oriented extracellular matrix/mesenchymal stem cell exosome bioink for osteochondral defect regeneration. *Theranostics*, 9(9): 2439–2459.

http://doi.org/10.7150/thno.31017

105. Ng CY, Chai JY, Foo JB, *et al.*, 2021, Potential of exosomes as cell-free therapy in articular cartilage regeneration: A review. *Int J Nanomed*, 16: 6749–6781.

http://doi.org/10.2147/ijn.S327059

106. Feng ZY, Zhang QY, Tan J, *et al.*, 2022, Techniques for increasing the yield of stem cell-derived exosomes: What factors may be involved? *Sci China Life Sci*, 65(7): 1325–1341.

http://doi.org/10.1007/s11427-021-1997-2

107. Yuan W, Wu Y, Huang M, *et al.*, 2022, A new frontier in temporomandibular joint osteoarthritis treatment: Exosome-based therapeutic strategy. *Front Bioeng Biotechnol*, 10: 1074536.

http://doi.org/10.3389/fbioe.2022.1074536